ISSN(Online) : 2319-8753
ISSN (Print) : 2347-6710

International Journal of Innovative Research in Science, Engineering and Technology

(An ISO 3297: 2007 Certified Organization)

Vol. 5, Issue 10, October 2016

Analysis of Combustion Furnace Performance using CFD

Gaurav Gupta[1], Dr.Girish Bagale[2]

PG Student, Dept. of Industrial Automation, MPSTME, NMIMS University, Mumbai, India

Professor, Dept. of Industrial Automation, MPSTME, NMIMS University, Mumbai, India

ABSTRACT: Processing of materials at high temperature often involves complex multi-phase fluid flow and heterogeneous chemical reactions. Due to the extreme temperature conditions existing within and around an industrial furnace, it is extremely difficult to measure the temperatures within a furnace at regular intervals during one operation cycle and thus find the characteristics of the furnace operation. Hence the industry needs an accurate method to estimate the flow characteristics of a furnace operation. Computational fluid dynamics (CFD) has become a very useful simulation tool to estimate the flow characteristics by improving process understanding. It can also simulate the effect of any changes made in the furnace for improving the efficiency of the furnace. The paper discusses the benchmarking of the CFD analysis followed by a CFD analysis on a heat treatment furnace.

KEYWORDS: Benchmarking using CFD, furnace, heat transfer, time steps, increasing efficiency of furnace

I. INTRODUCTION

A furnace is used to melt metals for casting or heat materials for change of shape (rolling, forging etc.) or change of properties (heat treatment). Based on the method of generating heat, furnaces are broadly classified into two types namely *combustion type (using fuels)* and *electric type*. Combustion furnaces based on the kind of combustion, it can be broadly classified as *oil fired, coal fired or gas fired.*

In Indian Industries, furnaces are operating below efficiency limits, causing large expenses. Performance Evaluation of a typical Furnace is the ratio of heat delivered to a material and heat supplied to the heating equipment.

The thermal efficiencies are low due to energy losses in different areas and forms. For most heating equipment, a large amount of the heat supplied is wasted in the form of exhaust gases.

These furnace losses include:

- Heat storage in the furnace structure
- Losses from the furnace outside walls or structure
- Heat transported out of the furnace by the load conveyors, fixtures, trays, etc.
- Radiation losses from openings, hot exposed parts, etc.
- Heat carried by the cold air infiltration into the furnace
- Heat carried by the excess air used in the burners.

ISSN(Online) : 2319-8753
ISSN (Print) : 2347-6710

International Journal of Innovative Research in Science, Engineering and Technology

(An ISO 3297: 2007 Certified Organization)

Vol. 5, Issue 10, October 2016

Bureau of Energy Efficiency, India studies typical thermal efficiencies as per following table.

Table 1 - Thermal Efficiencies for Common Industrial Furnaces

Furnace Type		Typical Thermal Efficiency (%)
Low Temperature furnaces		
a.	540-980 ^{0}C (Batch Type)	20-30
b.	540-980 ^{0}C (Continuous Type)	15-25
c.	Coil Anneal (Bell) radiant type	5-7
d.	Strip Anneal Muffle	7-12
High Temperature furnaces		
a.	Pusher, Rotary	7-15
b.	Batch forge	5-10
Continuous Kiln		
a.	Hoffman	25-90
b.	Tunnel	20-80
Ovens		
a.	Indirect fired (20-370 ^{0}C)	35-40
b.	Direct fired (20-370 ^{0}C)	35-40

*Ref.: Bureau of Energy Efficiency, India

To reduce the losses and improve the efficiency of the furnace we need to know certain parameters for estimating the flow within a furnace. But it difficult to measure all the parameters. For example, due to the extreme temperature conditions existing within and around an industrial furnace, it is very difficult to measure the temperatures within a furnace at regular intervals during one operation cycle. The flow characteristics can be estimated without actually measuring the parameters of the furnace using CFD. This paper shows how CFD can be used to stimulate the operation of the furnace so that the effective solution to increase the efficiency can be obtained without actually trying it at the furnace which involves high cost and affects the productivity.

II. LITERATURE SURVEY

A. CFD MODELING FUNDAMENTALS

ANSYS ICEM CFD provides advanced geometry acquisition, mesh generation, mesh optimization, and post-processing tools to meet the requirement for integrated mesh generation and post processing tools for today's sophisticated analyses. Maintaining a close relationship with the geometry during mesh generation and post-processing, ANSYS ICEM CFD is used especially in engineering applications such as computational fluid dynamics and structural analysis. ANSYS ICEM CFD provides a direct link between geometry and analysis.

In ANSYS ICEM CFD, geometry can be input from just about any format, whether from a commercial CAD design package, third party universal database, scan data or point data. Beginning with a robust geometry module

ISSN(Online) : 2319-8753
ISSN (Print) : 2347-6710

International Journal of Innovative Research in Science, Engineering and Technology

(An ISO 3297: 2007 Certified Organization)

Vol. 5, Issue 10, October 2016

which supports the creation and modification of surfaces, curves and points, ANSYS ICEM CFD's open geometry database offers the flexibility to combine geometric information in various formats for mesh generation. The resulting structured or unstructured meshes, topology, inter-domain connectivity and boundary conditions are then stored in a database where they can easily be translated to input files formatted for a particular solver. The Set of equations that are solves by Ansys CFX are unsteady Navier Stokes equations in their conservative form. These equations describe the processes of momentum, heat and mass transfer.[2] These partial differential equations were derived in the early nineteenth century and have no known general analytical solution but can be discretized and solved numerically. These equations can be given as:

$$\rho X - \frac{\partial p}{\partial x} + \mu\left(\frac{\partial^2 v_x}{\partial x^2} + \frac{\partial^2 v_x}{\partial y^2} + \frac{\partial^2 v_x}{\partial z^2}\right) = \rho\frac{Dv_x}{Dt} \quad (1)$$

$$\rho Y - \frac{\partial p}{\partial y} + \mu\left(\frac{\partial^2 v_y}{\partial x^2} + \frac{\partial^2 v_y}{\partial y^2} + \frac{\partial^2 v_y}{\partial z^2}\right) = \rho\frac{Dv_y}{Dt} \quad (2)$$

$$\rho Z - \frac{\partial p}{\partial z} + \mu\left(\frac{\partial^2 v_z}{\partial x^2} + \frac{\partial^2 v_z}{\partial y^2} + \frac{\partial^2 v_z}{\partial z^2}\right) = \rho\frac{Dv_z}{Dt} \quad (3)$$

where, *X*, *Y* and *Z* are the body forces in the *x*, *y* and *z* direction respectively is

ρ the density of fluid flowing

μ is the co-efficient of dynamic viscosity

v_x, v_y and v_z are velocities of flow in *x*, *y* and *z* directions respectively.[6]

B. HEAT TRANSFER

The temperature change in a body is governed by three physical processes: Convection Heat transfer, Latent heat transfer associated with mass transfer and radiation heat transfer. The Convective heat transfer Q_c is given in terms of Thermal Conductivity of fluid (λ), Temperatures of fluid and particle (T_G and T_p) and Nusselt number(N_u) by equation-

$$Q_c = \pi d\lambda N_u(T_G - T_p) \quad (4)$$

Nusselt number given by equation:

$$Nu = 2 + 0.6R_e^{0.5}\left(\frac{\mu C_P}{\lambda}\right)^{1/3} \quad (5)$$

where, C_P= Specific heat of fluid and μ= Fluid dynamic Viscosity.

For heat transfer associated with mass transfer the CFX uses following equation:

$$Q_M = \Sigma\frac{dm_c}{dt}V \quad (6)$$

Where sum is taken over all components of the particle for which the mass transfer is taking place. The latent heat of evaporation *V* is temperature dependent and is obtained from MATERIALS section in CFX for the liquid in the particle and its vapor. For heat transfer by radiation for particle with diameter d_p, uniform temperature T_p and emissivity $\varepsilon_p$the CFX uses equation:

$$Q_R = \varepsilon_p\pi d_p^2(I - \sigma n^2 T_p^2) \quad (7)$$

Where, *I* is the radiation intensity on the particle surface at the location of the particle, *n* is the refractive index of the fluid, and σ is the Stefan Boltzmann Constant.

ISSN(Online) : 2319-8753
ISSN (Print) : 2347-6710

International Journal of Innovative Research in Science, Engineering and Technology

(An ISO 3297: 2007 Certified Organization)

Vol. 5, Issue 10, October 2016

The Rate of change of temperature is then obtained by the equation (8) as:

$$\sum(m_C C_p)\frac{dT}{dt} = Q_C + Q_M + Q_R \quad (8)$$

Where, the sum in the equation (8) is taken over all the components of the particle including those not affected by mass transfer. [2]

C. MOMENTUM TRANSFER

Consider a discrete particle travelling in a continuous fluid medium. The forces acting on the particle that affect the particle are due to the difference in velocity between the particle and the fluid, as well as to the displacement of the fluid by the particle. The equation for it was derived by Basset, Boussinesq and Oseen for rotating frame. The Equation is:

$$m_p \frac{dU_p}{dt} = F_D + F_B + F_{VM} + F_P + F_{BA} \quad (9)$$

m_p is mass of the particle

$\frac{dU_p}{dt}$ is rate of change of velocity of the particle The equation (9) has following forces on the right side:

F_D = Drag force acting on the particle

= Buoyancy force due to gravity

F_B = Virtual Mass force - This is the force to accelerate the virtual mass of fluid in the volume occupied F_{VM} by the particle. This term is important when the displaced fluid mass exceeds the particle mass, such as in bubbles.

F_p = Pressure gradient force - This is the force applied on the particle due to the pressure gradient in the fluid surrounding the particle caused by fluid acceleration. It is only significant when the fluid density is comparable to or greater than the particle density.

F_{BA} = Basset force or history term which accounts for the deviation in flow pattern from the steady state.

The left hand side of the equation is modified due to special form of mass term called virtual mass term (This force is caused by the fact that the particle has to accelerate some of the surrounding fluid, leading to an additional drag.) The modified equation is given by eqn. as:

$$\frac{dU_p}{dt} = \frac{1}{m_p + \frac{C_{VM}}{2} m_F}(F_D + F_B + F'_{VM} + F_p) + \frac{1}{m_p} F_B \quad (10)$$

Only a part of the virtual mass term, F_{VM} remains on the right hand side. The particle and fluid mass values are given by:

$$m_F = \frac{\pi}{6} d_p^3 \rho_F \quad \text{and} \quad m_p = \frac{\pi}{6} d_p^3 \rho_p \quad (11)$$

Where d_p is particle diameter,
ρ_p and ρ_F are particle densities.
The ratio of original particle mass and the effective particle mass (due to the virtual mass term correction) is stored in equation given as:

$$R_{VM} = \frac{m_p}{m_p + \frac{C_{VM}}{2} m_F} = \frac{\rho_F}{\rho_F + \frac{C_{VM}}{2}\rho_F} \quad (12)$$

$$R_{VM} \quad \frac{\frac{C_{VM}}{2}\rho_F}{\rho_P + \frac{C_{VM}}{2}\rho_F}$$

ISSN(Online) : 2319-8753
ISSN (Print) : 2347-6710

International Journal of Innovative Research in Science, Engineering and Technology

(An ISO 3297: 2007 Certified Organization)

Vol. 5, Issue 10, October 2016

1- = (13)

Using R_{VM} the equation can be written as:

$$\frac{dU_p}{dt} = \frac{R_{VM}}{m_p}(F_D + F_B + F'_{VM} + Fp) + \frac{1}{m_p}F_R \quad (14)$$

Each term on the right hand side of equation (14) can potentially be linearized with respect to the particle velocity variable U_n , leading to the following equation for each term:

$$T = R + C_{lin}U_p \quad (15)$$

C_{lin} is the linearization co-efficient

There are a number of different solution methods that are used in CFD codes. The most common and the one on which CFX is based, is known as the finite volume technique. In this technique, the region of interest is divided into small sub-regions, called control volumes. The equations are discretized and solved iteratively for each control volume. As a result, an approximation of the value of each variable at specific points throughout the domain can be obtained. In this way, one derives a full picture of the behavior of the flow. [2]

III. BENCHMARKING

There are different solvers which simulates the flow characteristics using CFD. In order to achieve the accurate result, certain steps are to be followed such as giving correct input/output conditions, fluid properties. To make sure that our CFD analysis is accurate, a run is conducted on a pre-analyzed furnace. This furnace has been analyzed using known and tested CFD techniques in the past and is referred in a published and documented paper. This step is essential as it allows performing a run on our industrial furnace with the confidence that the steps followed are accurate and will yield good results. This step is known as “Benchmarking”.

Benchmarking involves the following vital steps:

- Selection of a tested furnace from a published paper and study it.
- Start CFD runs on the selected furnace in software package and using a selected method.
- Compare results obtained with the results published in the paper. If found matching, the selected method is acceptable.

CFD analysis for this paper has been done using ANSYS-CFX solver and ICEM-CFD as a meshing tool.

ISSN(Online) : 2319-8753
ISSN (Print) : 2347-6710

International Journal of Innovative Research in Science, Engineering and Technology

(An ISO 3297: 2007 Certified Organization)

Vol. 5, Issue 10, October 2016

IV. EXPERIMENTATION

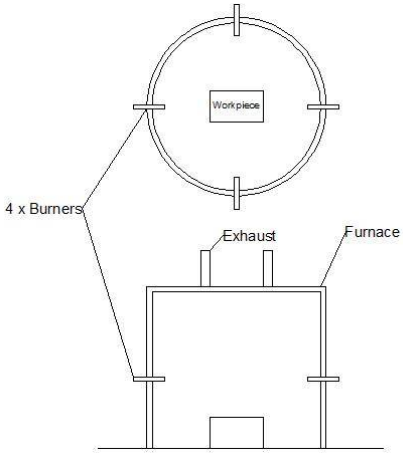

Fig 1: Furnace Design and Geometry

Fig. 1 shows a heat treatment furnace was simulated by using CFD to investigate thermal performance of the furnace and the heating process of the metal pieces. The furnace is used to heat treat dredging pumps and impellers to obtain the required microstructure and mechanical properties through stress relief, annealing, hardening and tempering. Since the temperature evolution inside the metal piece cannot be tracked in practice, CFD simulation provides a useful tool to predict the temperature evolution within the metal pieces during the heat treatment.
The current CFD model consists of turbulent combustion, thermal radiation, and conjugate heat transfer. Heated air at 668°C is passed through burners over the impeller. The total time for simulation carried out is 5 hour in time steps of 20 minutes. The main purpose of this paper is to predict the temperature evolution within the metal pieces during the heat treatment and validate the results obtained with values from the paper.

1. Furnace Design and Geometry

- Furnace dimension: Diameter x Height - 3.76 m x 3.5 m (Volume = 156 m^2)
- Burner diameter and location: 0.1 m in diameter, 1.5m from furnace bottom.
- Impeller dimensions: Outer Diameter x Inner Diameter x Height - 1.5 x 0.5 x 0.6

2. Model Geometry

The geometry created in ICEM is shown in the form of a wireframe model. The impeller is kept inside the furnace but is kept as a separate solid domain to enable the solver to interpret is as a separate entity. A simplified cad model of the impeller is used and the impeller is kept slightly above ground level in the furnace to facilitate use of supports in application.

3. Mesh Parameters

Meshing was done in ICEM-CFD. The fluid and solid domain were meshed separately. This was done to ensure that while applying boundary conditions, the solver can differentiate fluid and solid domains. Different mesh sizes were given to different parts based on their size. The mesh parameters are:

- Tetrahedral mesh is used.
- Mesh size is 0.1 for the furnace volume, 0.01 for the inlet and outlet pipes, and 0.05 for the impeller.
- A prism layer is kept around the impeller towards the fluid boundary. Prisms are of height 0.001 with a height ratio of 1.1. Three such layers are kept.

ISSN(Online) : 2319-8753
ISSN (Print) : 2347-6710

International Journal of Innovative Research in Science, Engineering and Technology

(An ISO 3297: 2007 Certified Organization)

Vol. 5, Issue 10, October 2016

Prism layer helps in getting accurate reading around the impeller. Also keeping a good prism layer helps the solver to achieve a good y-plus value.

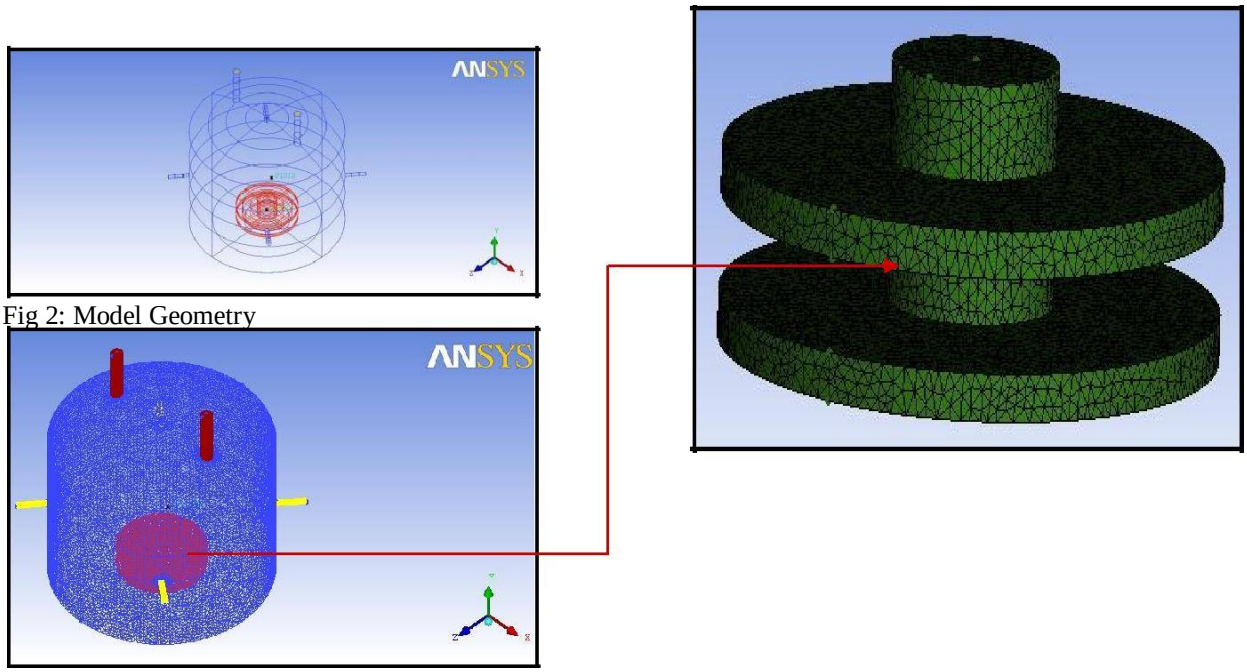

Fig 2: Model Geometry

Fig 3: Mesh Parameters

4. Assumptions: The following assumptions have been taken while performing a solver run.

Table 2: Assumptions

No combustion	
Analysis type	: Transient
Working fluid	: Air at 668°C
Heat Transfer Model	: Thermal Energy
Turbulence Model	: K-Epsilon

Impeller is assumed to be continuous solid

Domain assumed is stationary

Fluid Properties:

Viscosity	1.09e-5 Ns/m ^{2}
Specific Heat	1004.4 J/kg-K
Conductivity	0.032411 W/mK
Thermal Expansivity	0.003356/K
Density	1.2 Kg/m ^{3}

ISSN(Online) : 2319-8753
ISSN (Print) : 2347-6710

International Journal of Innovative Research in Science, Engineering and Technology

(An ISO 3297: 2007 Certified Organization)

Vol. 5, Issue 10, October 2016

5. Boundary Conditions

The boundary conditions following were applied as given in the paper. The above mentioned assumptions were applied to the boundary conditions and then given input to the solver. Mass flow rate is given as combined and the solver divides it among the available inlet pipes.

Table 3 Boundary Conditions

INLET	Mass Flow Rate – 0.37 kg/s
	Boundary Type – Inlet
	Flow Regime – Subsonic
	Turbulence - 5% Medium Intensity
WALL	No-Slip type
	Adiabatic
OUTLET	Boundary Type- Outlet
	Turbulence- Medium Intensity

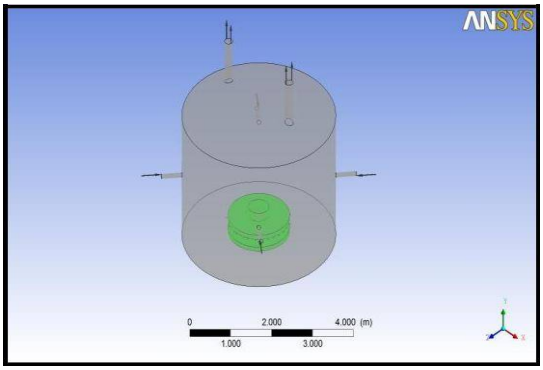

Fig 4: Boundary Conditions

V. RESULTS AND DISCUSSION

A. GENERAL GAS FLOW PATTERN

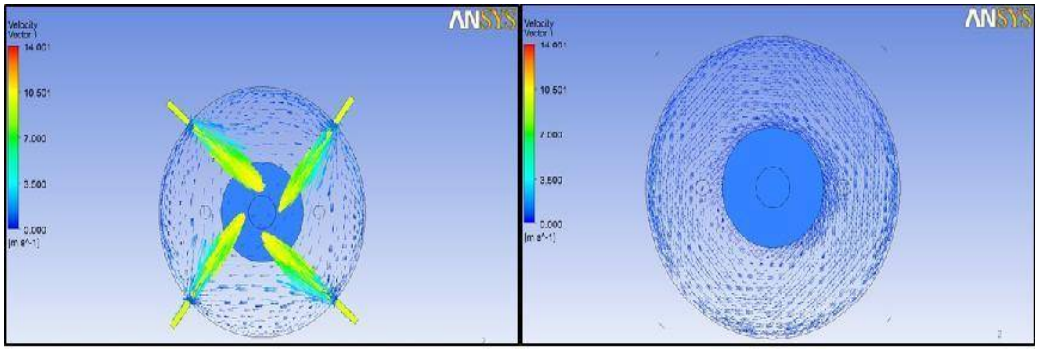

Fig 5: Gas flow pattern

As is described earlier, there are four oil burners installed slightly above the top surface of the impeller. The two opposing burners have a small angle of 6.5° so that the flame jets do not meet in the center of the furnace, and more

ISSN(Online) : 2319-8753
ISSN (Print) : 2347-6710

International Journal of Innovative Research in Science, Engineering and Technology

(An ISO 3297: 2007 Certified Organization)

Vol. 5, Issue 10, October 2016

stable and slightly rotating flames are formed. Figure 5 shows the general gas flow pattern obtained from the final model at three different cross sections. From Figure 5(a), 5(b) it can be seen that the jets from the four burners form a counter clockwise rotating flow. This rotating flow extends from the burner level to the top of the furnace upward and to the bottom of the furnace downwards. From Figure 5(c) it can be seen that near the center of the furnace between the two pair of burners, a downward gas flow is formed, which is ended near the impeller top-surface. Below the impeller the velocity is much lower, which is not efficient for the heating process of the lower part of the impeller.

B. TEMPERATURE EVOLUTION RESULTS OF THE JOB

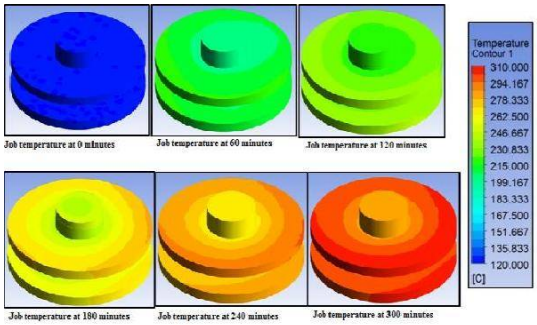

Fig 6: Temperature Evolution results of job

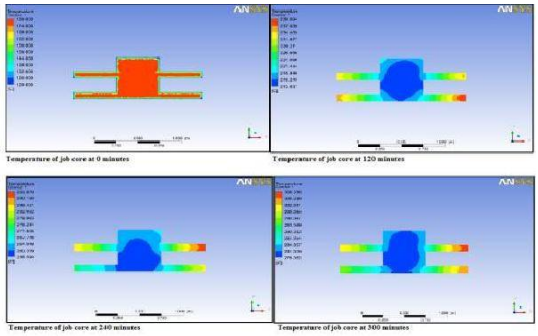

Fig 7: Temperature evolution at job core

C. TEMPERATURE EVOLUTION RESULTS AT THE JOB CROSS SECTION:

Fig.7 illustrates a temperature contours from the final transient simulation model. Due to the limited space in the paper, only a few time steps were chosen from the 15 time steps (time 0 – 5 hours). From these snap-shots, the heating processes of the furnace space and the impeller can be clearly seen along the heating process. The temperature of the impeller is higher on the top. The lower parts of the impeller have some delay in temperature increase. As was mentioned before the heating of lower parts is slow due to slower flow at the lower parts of the furnace. Hence the flow patterns support the temperature results.

D. THERMOCOUPLES IN FURNACE SPACE:

As per SAE standard AMS 2750D, 9 thermocouples are used for temperature measurement. The variation of temperature at the individual thermocouples is shown with the progress in time. The points are monitored continuously during the progress of solution.
The placement of the points in two views is shown in fig. 8. The points are placed at 0.5, 1.5, and 2 meteres from the furnace level. Hence they lie at job and burner level and space. Four such points are placed at 90 degrees to each other.

ISSN(Online) : 2319-8753
ISSN (Print) : 2347-6710

International Journal of Innovative Research in Science, Engineering and Technology

(An ISO 3297: 2007 Certified Organization)

Vol. 5, Issue 10, October 2016

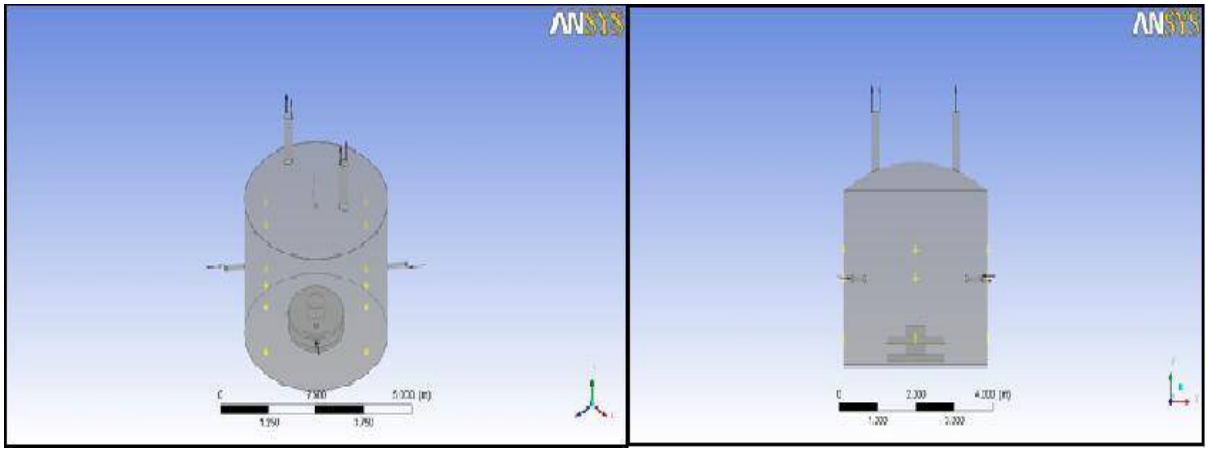

Fig 8: Placement of points in space

VI. CONCLUSION

The results obtained by simulation are documented as above. The heating profile was reasonably predicted by the simulation. Through the CFD simulation, not only the surface temperature could be properly predicted, but also the temperature within the metal components could be simulated. The latter is crucial for the heat treatment process, but is not possible to measure directly in practice. The results obtained by us are found to be in acceptable limit (± 5%). This indicates and extremely accurate range. Hence it is proved that method of analysis used for the current paper is accurate and can now be applied to an industrial furnace.

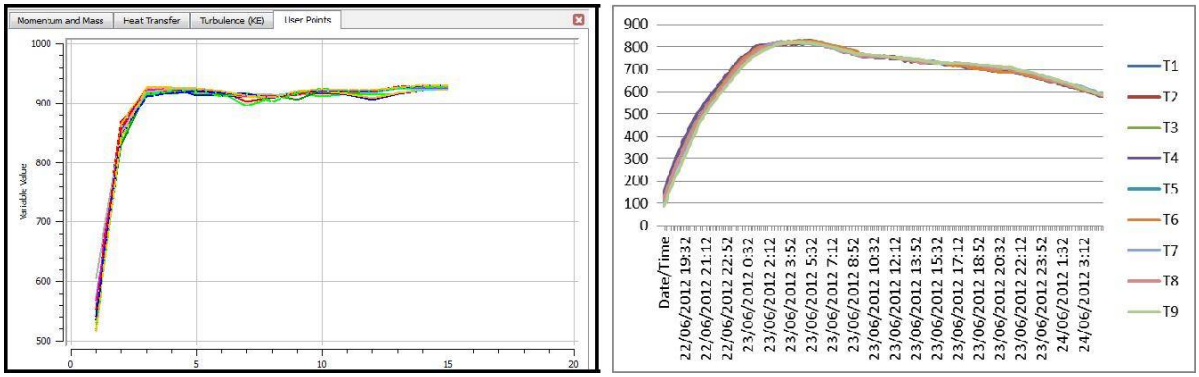

Fig 9: Variation of temperatures (a) Simulation results, (b) Actual results

REFERENCES

1. Blazek , Computational fluid dynamics: principles and applications, 2001 (Amsterdam, Elsevier Publications)
2. ANSYS Inc., Ansys CFX.13 Theory Guide, 2010
3. R. W. Lewis, P. Nithiarasu, K. N. Seetharamu, Fundamentals of the finite element method for heat and fluid flow, 2008 (New Jersey, John Wiley & Sons, Ltd)
4. M. M. Rathore , Engineering heat and mass transfer, 2006 (New Delhi, LaxmiPrakashan)
5. A. Trinks, M. H. Mawhinney, R. A. Shannon, R. J. Reed and J. R. Garvey, Industrial furnaces, 2004 (New Jersey, John Wiley & Sons, Inc.)
6. T. J. Chung, Computational Fluid Dynamics, 2003 (Cambridge, Cambridge University Press)
7. Kang , R. Purushothaman, Y. Rong A. K. Singh and L. Zhang , Computer Aided Heat Treatment Planning System for Quenching and

ISSN(Online) : 2319-8753
ISSN (Print) : 2347-6710

International Journal of Innovative Research in Science, Engineering and Technology

(An ISO 3297: 2007 Certified Organization)

Vol. 5, Issue 10, October 2016

Tempering , Integrated Computational Materials Engineering: Lessons from Many Fields, TMS (The Minerals, Metals and Materials Society), 2007

8. C. A. García, J. C. Moreno-Piraján and F. Sánchez, Simulation and Flow Analysis for a Brick Furnace, Electronic Journal Of Environmental, Agriculture and Food Chemistry,5, 2006
9. A. J. Jang and S. W. Kim , An Estimation of a Billet Temperature during Reheating Furnace Operation, International Journal of Control, Automation, and Systems, 1(5), 2007, 43-50
10. R. A. de Jong , M. A. Reuter and Y. Yang, Use of CFD to Predict the Performance of a Heat Treatment Furnace, Fourth International Conference on CFD in the Oil and Gas, Metallurgical & Process Industries SINTEF / NTNU Trondheim, Norway, 2005
11. R. Boom, J. R. Post, M. A. Reute, E. Scheepers, Y. Yang and B. Zhou, Computational Fluid Dynamics Simulation of Pyro metallurgical Processes, Fifth International Conference on CFD in the Process Industries CSIRO, Melbourne, Australia , 13-15, 2006
12. P. Diwakar , V. Mehrotra, , R. Vallavanatt, Troubleshooting Furnace Operations using Computational Fluid Dynamics (CFD), Proceedings of ASME-PVP' 04 5th International Bi-Annual ASME/JSME Symposium on Computational Technology for Fluid/Thermal/Chemical/Stressed Systems with Industrial Applications an Diego (La Jolla), California, 2004
13. E. H. Chui , Applications Of CFD Modeling In Canadian Industries, Fourth International Conference on CFD in the Oil and Gas, Metallurgical & Process Industries, SINTEF / NTNU Trondheim, Norway, 2005
14. R. Mehta and S. Sahay, Heat Transfer Mechanisms and Furnace Productivity During Coil Annealing: Aluminum vs. Steel, ASM International, 2008
15. Doe, Fundamentals handbook thermodynamics, heat transfer and fluid flow (Volume 1, 2 and 3, U.S. Department of Energy FSC-6910, Washington, D.C. 20585)